ФИЗИКА ЭЛЕМЕНТАРНЫХ ЧАСТИЦ И АТОМНОГО ЯДРА
2007. Т. 38. ВЫП. 2

ISOSPIN DEPENDENCE OF THE SPIN–ORBIT SPLITTING IN NUCLEI

V. I. Isakov[*]

Petersburg Nuclear Physics Institute, Gatchina, Russia

An analysis has been made of experimental data on level spectra, single-nucleon transfer reactions near closed shells, and data on polarization effects in charge-exchange (p, n) reactions between isoanalogous states of nuclei with even A. The analysis makes it possible to conclude that there is a significant difference between the spin–orbit splittings of neutrons and protons in identical orbitals. This conclusion is confirmed in the framework of different theoretical approaches.

В работе приведен анализ экспериментальных данных по спектрам одночастичных уровней, реакциям однонуклонной передачи в ядрах вблизи заполненных оболочек и данных по поляризационным эффектам в зарядово-обменных (p, n)-реакциях, происходящих между изоаналоговыми уровнями ядер с четными значениями массовых чисел A. Результаты анализа позволяют сделать вывод о существовании заметной разницы между спин-орбитальными расщеплениями нейтронов и протонов, находящихся на идентичных орбиталях. Это различие объясняется в рамках различных теоретических подходов.

PACS: 21.10.Hw

INTRODUCTION

The energy spectrum of mean-field single-particle states and, in particular, their spin–orbit splittings are among the most important features of nuclei that underlie all microscopic descriptions of nuclear structure. In particular, spin–orbit splittings determine, among the other things, the shell properties of nuclei both near and far from the closed shells. While the global characteristics of the spin–orbit splittings are well known, this cannot be said about the isotopical dependence of the splitting.

The best way to determine such a dependence from the experiment is to intercompare proton and neutron spin–orbit splittings of the *same* (with similar values of the *n,l* quantum numbers) spin–orbit doublets in the neighbouring odd-neutron $(N \pm 1, Z)$ and odd-proton $(N, Z \pm 1)$ nuclei, where both N and Z are even, while $N \neq Z$. The last condition is necessary as in the case of $N = Z$

[*]E-mail: visakov@thd.pnpi.spb.ru; Vadim.Isakov@thd.pnpi.spb.ru

both the aforementioned splittings are equal due to the isobaric symmetry of nuclear forces.

When determining the values of single-particle energies from the experiment, one must take into account the problem that, in actual nuclei, single-particle mode is mixed with the more complicated excitation modes, with the result that there occurs a redistribution of the single-particle strength (the so-called configuration mixing). This effect is rather small in nuclei of the *magic nucleus* $\pm$ *nucleon* type if the single-particle gap is large as in the case for «good» magic nuclei like ^{132}Sn and ^{208}Pb, but the spreading of single-particle states over levels belonging to the *quasiparticle plus phonon* type may occur here as well. In the case of a small energy gap, configuration mixing may become very strong. Here, stripping (pick-up) reactions characterized by a seazable cross section excite not only single-particle states peculiar to, for example, nuclei of the *magic nucleus* $\pm$ *nucleon* type but also levels with quantum numbers J^π that correspond to single-particle states on the other side of the Fermi level. In any case, an additional averaging procedure is required for extracting *true* single-particle levels from experimental data.

Below we give a consistent validation [1] of the procedure for determining single-particle energies that is based on the precise formulas and on the experimental data concerning one-nucleon pick-up and stripping reactions and the values of one-nucleon separation energies. By using this procedure we determine the «true» single-particle proton energies in the regions of magicity close to ^{48}Ca, ^{208}Pb, and ^{132}Sn. The obtained values of spin–orbit splittings show the isotopic dependence of spin–orbit splitting in nuclei. The existence of this splitting is confirmed [2] by the theoretical analysis performed in the framework of different approaches. In conclusion we present additional arguments [3] in favour of such a dependence, that is based on the data concerning the (p, n) charge-exchange reactions with excitation of the isoanalogous states in the final nuclei.

1. GENERAL RELATIONS FOR DETERMINING SINGLE-PARTICLE MEAN-FIELD ENERGIES FROM EXPERIMENTAL DATA ON DIRECT REACTIONS OF ONE-NUCLEON TRANSFER

Here we describe the procedure for determining single-particle energies from experimental data on the basis of, for example, the Hamiltonian for two-body forces in the second-quantization representation. We have

$$\hat{H} = \sum_{i,k} \langle i|\hat{t}|k\rangle a_i^+ a_k + \frac{1}{4} \sum_{i,k,\ell,m} {}_a\langle ik|\hat{\vartheta}|\ell m\rangle_a a_i^+ a_k^+ a_m a_\ell, \tag{1}$$

where ${}_a\langle ik|\hat{\vartheta}|\ell m\rangle_a = \langle ik|\hat{\vartheta}|\ell m\rangle - \langle ik|\hat{\vartheta}|m\ell\rangle$ is the antisymmetric matrix element for the pair interaction $\hat{\vartheta}(x_1 x_2) = \hat{\vartheta}\,(\mathbf{r_1}, \hat{\boldsymbol{\sigma}}_1, \hat{\boldsymbol{\tau}}_1, \mathbf{r_2}, \hat{\boldsymbol{\sigma}}_2, \hat{\boldsymbol{\tau}}_2)$, while $\hat{t}$ is the single-

particle kinetic-energy operator. We further introduce the auxiliary quantity

$$\hat{Q}_\alpha = \left\{a_\alpha, [\hat{H}, a_\alpha^+]\right\} \equiv a_\alpha \hat{H} \cdot a_\alpha^+ - a_\alpha \cdot a_\alpha^+ H + H a_\alpha^+ \cdot a_\alpha - a_\alpha^+ H \cdot a_\alpha, \quad (2)$$

where $[\hat{G}, \hat{F}]$ and $\{\hat{G}, \hat{F}\}$ are, respectively, the commutator and anticommutator of the operators $\hat{G}$ and $\hat{F}$. On the one hand, we average $\hat{Q}_\alpha$ taken in the form (2) over the ground state $|A;(0)\rangle$ of even–even nucleus containing A particles, expanding intermediate states in a complete set of wave functions for the systems of $(A+1)$ and $(A-1)$ particles. On the other hand, we directly calculated $\hat{Q}_\alpha$ by means of (1) with a subsequent averaging. As a result, we arrive at the exact relation

$$\begin{aligned}\sum_{a\in(A+1)} &[B_A(\mathrm{gr.st.}) - B_{A+1}(\mathrm{gr.st.}) + E_a^{\mathrm{exc}}]\, s_{a\alpha}^{(+)} + \\ &+ \sum_{a'\in(A-1)} [B_{A-1}(\mathrm{gr.st.}) - B_A(\mathrm{gr.st.}) - E_{a'}^{\mathrm{exc}}]\, s_{a'\alpha}^{(-)} = \\ &= \langle\alpha|\hat{t}|\alpha\rangle + \langle A;(0)| \sum_{i,k} {}_a\langle\alpha i|\hat{\vartheta}|\alpha k\rangle_a a_i^+ a_k |A;(0)\rangle, \quad (3)\end{aligned}$$

where

$$\begin{aligned} s_{a\alpha}^{(+)} &= |\langle A+1;(a)|a_\alpha^+|A;(0)\rangle|^2, \\ s_{a'\alpha}^{(-)} &= |\langle A-1;(a')|a_\alpha|A;(0)\rangle|^2. \end{aligned} \quad (4)$$

Here, $|A;(0)\rangle$ is the vector of the ground state of an initial even–even nucleus; $|A+1;(a)\rangle$ and $|A-1;(a')\rangle$ are, respectively, the vectors of $\{a\}$ and $\{a'\}$ states of the nuclei containing $(A+1)$ and $(A-1)$ nucleons with allowance for fragmentation effects; $E_{a,a'}^{\mathrm{exc}}$ are the corresponding excitation energies ($E_{a,a'}^{\mathrm{exc}} = 0$ for the ground states); and $B_{A,A\pm1}$ are the binding energies in the ground states of the corresponding nuclei. In (3) and (4), the values of J^π for the $\{a\}$ and $\{a'\}$ states are identical to those for the single-particle state $\{\alpha\}$.

The quantities $s_{a\alpha}^{(+)}$ and $s_{a'\alpha}^{(-)}$ represent the spectroscopic factors of states, specifying the fraction of the single-particle state $\{\alpha\}$ in the complex states $\{a\}$ or $\{a'\}$. They are normalized by the relation

$$\sum_{a\in(A+1)} s_{a\alpha}^{(+)} + \sum_{a'\in(A-1)} s_{a'\alpha}^{(-)} = 1, \quad (5)$$

which is exact and follows from the anticommutation relation for the single-particle fermion operators,

$$a_\alpha^+ a_\beta + a_\beta a_\alpha^+ = \delta_{\alpha\beta}. \quad (6)$$

It should be noted that, in the literature, use is often made of the spectroscopic factors $\tilde{s}^{(\pm)}_{a(a')\alpha} = (2j_\alpha + 1)s^{(\pm)}_{a(a')\alpha}$ normalized to $(2j_\alpha + 1)$. In the present study, we everywhere employ the normalization condition (5).

Now we consider the expression on the right-hand side of Eq. (3). This expression has the meaning of a single-particle energy. We will discuss this issue in more detail. We introduce the field operators $\Psi^+ = \sum_\beta \varphi^*_\beta(x)a^+_\beta$, where $\varphi_\beta(x)$ are functions of a complete single-particle set, which is considered to be arbitrary for the time being. The second term in the expression on the right-hand side of Eq. (3) can then be recast into the form

$$\iint dx_1 dx_2 [\rho_\alpha(x_1x_1)\rho(x_2x_2) - \rho_\alpha(x_1x_2)\rho(x_2x_1)]\hat{\vartheta}(x_1x_2), \tag{7}$$

where

$$\begin{gathered}\rho_\alpha(x_1x_2) = \varphi^*_\alpha(x_1)\varphi_\alpha(x_2),\\ \rho(x_1x_2) = \langle A;(0)|\Psi^+(x_1)\Psi(x_2)|A;(0)\rangle.\end{gathered} \tag{8}$$

Here the quantities ρ_α and ρ, which are diagonal in the indices x_1 and x_2, are, respectively, the density of the single-particle state $\{\alpha\}$ and the exact matter density of the core nucleus. It can easily be seen that, in terms of a diagram technique, expression (7) represents the diagonal matrix element of the «single-particle» mass operator $\hat{\Sigma}_{\mathrm{s.p}}$ for the single-particle Green function G, that in the (x,t) representation has the form

$$G(x,t;x',t') = -i\langle A;(0)|\hat{T}\{\Psi(x,t),\Psi^+(x',t')\}|A;(0)\rangle, \tag{9}$$

where $\Psi(x,t)$ are field operators $\Psi(x)$ in the Heisenberg representation and $\hat{T}$ is the chronological-ordering operator. The mass operator corresponding to (7) can be represented as a sum of two diagrams in Fig. 1, having the form similar to that of the mass operator in the Hartree–Fock approximation. However, the single-particle Green function $G(\varepsilon)$, which is the Fourier transform of (9) with respect to the variable $(t - t')$ and which is depicted by a thick line in Fig. 1, is *exact* since the quantity $\rho(x_1x_2)$ is defined as an average over the *true* ground state of the system containing A particles. Actually, this means that the definition of $\rho(x_1x_2)$ according to (8) involves, in addition to diagrams similar to those in Fig. 2, *a* and *b* (appearing in the Hartree–Fock approximation), diagrams belonging to the types in Fig. 2, *c* and *d*, corresponding to certain effects beyond the approximation in question, and reflecting the contribution of ground-state correlations. It is appropriate to mention here the study of Birbrair and Ryazanov [4],

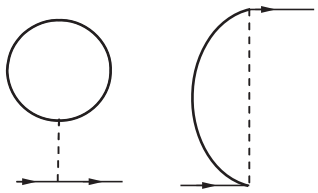

Fig. 1. Mass operator corresponding to expression (7)

who derived relation (3) from Dyson's equation and the spectral expansion of the single-particle Green function. Here, it is important that the single-particle energy corresponding to the mass operator independent of the input energy of the Green function $G_\alpha(\varepsilon)$ appeared on the right-hand side of the formula analogous to (3) in [4]. It can easily be shown that the mass operator corresponding to expressions (7) and (8), which is displayed in Fig. 1, does not depend on ε, so that it does not involve fragmentation effects and corresponds to «true» single-particle states $\{\alpha\}$ diagonalizing the operator $\hat{t} + \hat{\Sigma}_{\mathrm{s.p}}$.

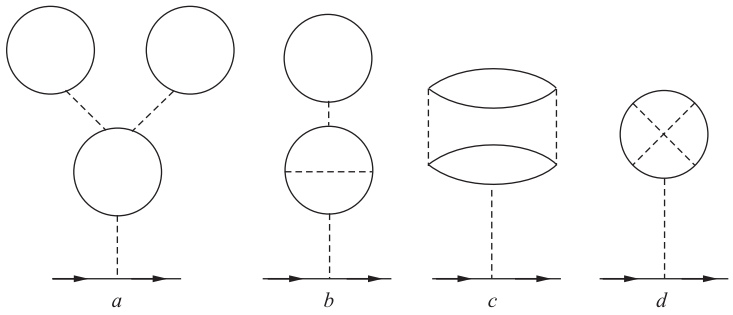

Fig. 2. Contributions to the mass operator independent of ε that are taken into account (a, b) and disregarded (c, d) in the Hartree–Fock approximation

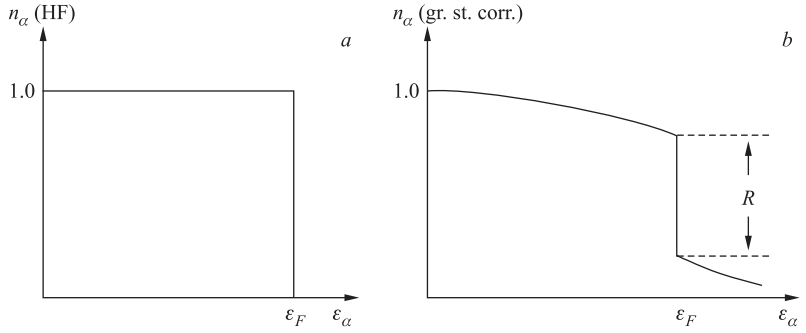

Fig. 3. Particle distribution n_α in the absence (a) and in the presence (b) of the ground-state correlations

If, instead of the *true* ground state $|A;(0)\rangle$ of nucleus A, we use the ground-state vector of the Hartree–Fock approximation (that is, the Slater determinant) $|A;(0)\rangle_{\mathrm{HF}}$ — it corresponds to a Fermi step of height equal to unity in the space of occupation numbers $n_\alpha = {}_{\mathrm{HF}}\langle A;(0)|a_\alpha^+ a_\alpha|A;(0)\rangle_{\mathrm{HF}}$ (see Fig. 3, *a*) — and if, for $\{\alpha\}$, we use the Hartree–Fock eigenfunctions, then $a_i^+|A;(0)\rangle_{\mathrm{HF}} = 0$ for

$\varepsilon_i < \varepsilon_F$ and $a_k|A;(0)\rangle_{\rm HF} = 0$ for $\varepsilon_k > \varepsilon_F$. The right-hand side of Eq. (3) will then take the form

$$\langle\alpha|\hat{t}|\alpha\rangle + \sum_{i;\ \varepsilon_i<\varepsilon_F} {}_a\langle\alpha i|\hat{\vartheta}|\alpha i\rangle_a \equiv \varepsilon_\alpha(\mathrm{HF}). \tag{10}$$

However, the left-hand sides of Eqs. (3) and (5) will involve only $s^{(+)}$ or $s^{(-)}$ components.

It should be noted that the actual ground state involves correlations; even in the absence of superfluidity, the respective particle distribution n_α, which is displayed in Fig. 3, *b*, has a jump at $\varepsilon = \varepsilon_F$, this jump $R < 1$ being equal to the residue of the Green function G (Migdal's theorem, [5]). As a result, $a_i^+|A;(0)\rangle \neq 0$ for $\varepsilon_i < \varepsilon_F$ and $a_k|A;(0)\rangle \neq 0$ for $\varepsilon_k > \varepsilon_F$, while expressions (3) and (5) involve both $s^{(+)}$ and $s^{(-)}$ terms.

In treating experimental data, the single-particle factors s are determined by analyzing direct reactions of single-particle stripping and pick-up. Now we consider this point in more detail. Suppose that the target nucleus is an even–even nucleus featuring the quantum numbers $J^\pi = 0^+$ and $T = T_Z = T_0 = \dfrac{N-Z}{2}$. Summation in (3) and (5) covers all possible states (complete set) — in particular, all possible isospin states. By explicitly including isospin variables, we can reduce expressions (4) to the form

$$s^{(+)}_{a\alpha} = \left|\langle A+1;(a,T_f,T_{zf})|a^+_{\alpha,t=\frac{1}{2}\,tz}|A;(\text{gr. st.},T_0,T_z=T_0)\rangle\right|^2 = \left[C^{T_fT_{zf}}_{\frac{1}{2}\,tz,T_0T_0}\right]^2 S(a,\alpha,T_f,T_0), \tag{11}$$

$$s^{(-)}_{a'\alpha} = \left|\langle A-1;(a',T_f,T_{zf})|a_{\alpha,t=\frac{1}{2}\,tz}|A;(\text{gr. st.},T_0,T_z=T_0)\rangle\right|^2 = \left[C^{T_fT_{zf}}_{\frac{1}{2}\,-tz,T_0T_0}\right]^2 S(a',\alpha,T_f,T_0), \tag{12}$$

where the quantities S are independent of the isospin projection.

2. DETERMINATION OF THE ENERGIES OF SINGLE-PARTICLE STATES IN THE VICINITY OF THE ^{48}Ca, ^{208}Pb, AND ^{132}Sn NUCLEI

The diagram describing the excitation of the levels of interest in the vicinity of the ^{48}Ca nucleus can be represented in the form displayed in Fig. 4, where $T_< = T_0 - 1/2$ and $T_> = T_0 + 1/2$. This figure shows that, in order to determine the energies of single-particle orbitals, it is necessary, in analyzing data

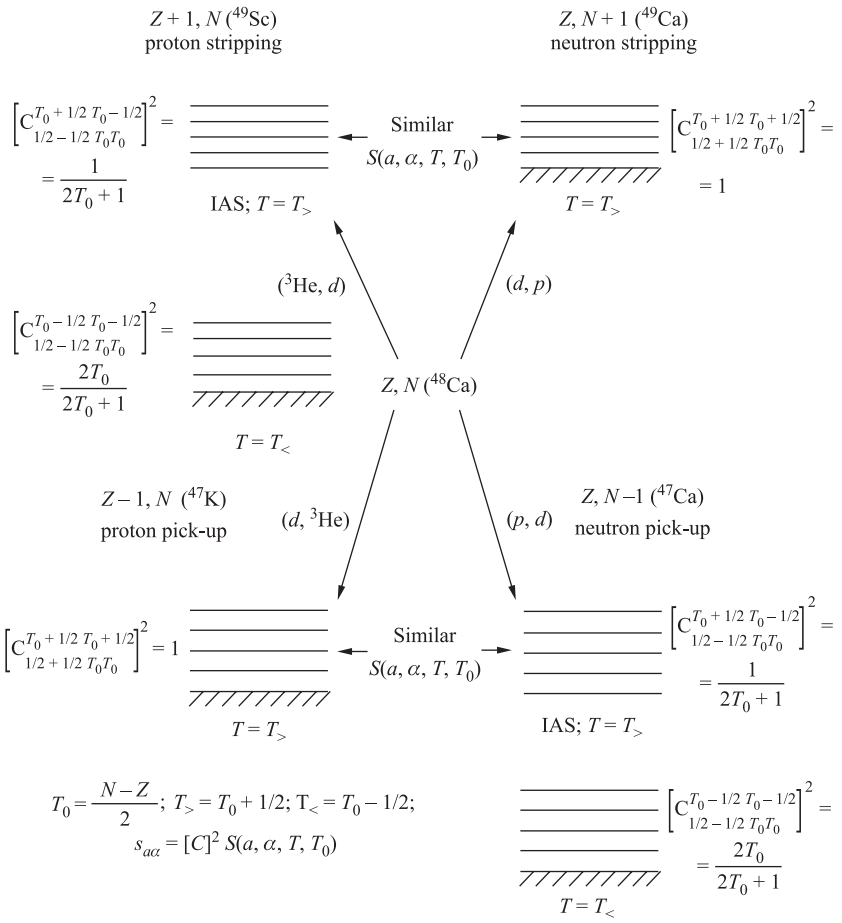

Fig. 4. Diagram of the excitation of levels in the vicinity of the ^{48}Ca nucleus in single-particle transfer reactions

on reactions of proton stripping and neutron pick-up, to take into account in (3) highly excited analogous states of $T = T_>$, for which experimental information is not always available. By employing isobaric symmetry, one can borrow, however, the corresponding isospin-reduced spectroscopic factors $S(a, \alpha, T_>, T_0)$ from the reactions involving neutron stripping and proton pick-up and leading to low-lying states of the neighbouring isobaric nuclei. At the same time, it should be borne in mind that the contribution of transition to the analogous states of final nuclei is suppressed by the factor $1/(2T_0+1)$, which is equal to $1/45$ for the target nucleus ^{208}Pb, but which increases considerably for light nuclei (1/9 for ^{48}Ca). Another

distinction of the region around $A \sim 48$ from the regions around $A \sim 208$ and $A \sim 132$ is that, in the ^{48}Ca nucleus, the shells are relatively weak, which is manifested in that direct reactions of one-nucleon transfer excite, in odd nuclei, low-lying states with quantum numbers J^π which are typical of single-particle states belonging to «alien» shells on the other side of the Fermi surface. The aforementioned indicates that both the $T_>$ states of odd nuclei and ground-state correlations must be taken into account in determining ε_α in the vicinity of the ^{48}Ca nucleus.

Since we are interested primarily in spin–orbit splitting, we will consider in detail the procedure for determining the energies of $\{1d\}$ levels, clarifying one important point in advance.

The quantities $s^{(\pm)}$ appearing in expressions (3) and (5) are determined by analyzing experimental data on direct nuclear reactions. In doing this, there arises a natural uncertainty associated both with experimental errors and with the accuracy of a theoretical description (usually, within the distorted-wave Born approximation) of stripping (pick-up) processes; as a result, the right-hand side of (5) may become different from unity even in a complete experiment. In actual calculations, we therefore modified expression (3) by means of the substitution $s^{(\pm)}_{i(i')} \to s^{(\pm)}_{i(i')} / \left(\sum_k s^{(+)}_k + \sum_{k'} s^{(-)}_{k'} \right)$, going over to normalized s factors. It should be noted that the electronic database from [6] and references therein (if necessary) were used as a main source of experimental data in determining the spectroscopic factors. The nuclear binding energies were borrowed from [7].

Now we consider the neutron hole state $\{\nu 1d_{5/2}\}$. Figure 4 shows that a correct determination of single-particle energies here requires taking into account not only low-lying but also highly excited isobaric analogous states in ^{47}Ca at excitation energies higher than 12 MeV (in the ^{47}Ca nucleus, the lowest $T_>$ state, which is the isoanalog of the $1/2^+$ ground state of the ^{47}K nucleus, has the energy of 12.73 MeV). From experiments, it follows that the $\{\nu 1d_{5/2}\}$ state of the ^{47}Ca nucleus is strongly fragmented. Up to the excitation energy of 11 MeV, the respective (^{3}He, α) reaction exhibits 46 $5/2^+$ ($T = T_<$) levels characterized by $\sum_{i'} s^{(-)}_{i'} = 0.607$ and $\sum_{i'} s^{(-)}_{i'} E_{i'} = 4.798$ MeV. The lowest $5/2^+$ isoanalog of the ^{47}K nucleus has $E = 16.12$ MeV and $s^{(-)} = 0.06$ and corresponds to $5/2^+$ level of ^{47}K at $E = 3.43$ MeV. At the same time, the reaction ^{48}Ca(d, ^{3}He)^{47}K exhibits a variety of other low-lying ($E < 9$ MeV) $5/2^+$ states that are hardly seen, because of a small cross section (in particular, due to the isotopic factor of $= 1/9$), as higher $5/2^+$ isoanalogous states of the ^{47}Ca nucleus. We can rescale the energies of low-lying $5/2^+$ states of the ^{47}K nucleus to those of the $5/2^+$ isoanalogous states in the ^{47}Ca nucleus, assuming that the relative values of $s^{(-)}$ for various isoanalogs in ^{47}Ca are identical to those for low-lying $5/2^+$ states in

^{47}K. After the normalization to the well-known experimental value of $s^{(-)}$ for the $5/2^+$ state at $E = 16.12$ MeV, we then obtain the following values for the $T_>$ levels in the ^{47}Ca nucleus: $\sum_{k'} s_{k'}^{(-)} = 0.231$ and $\sum_{k'} s_{k'}^{(-)} E_{k'} = 4.272$ MeV. As a result, we arrive at $\varepsilon_{\nu 1d_{5/2}} = -20.76$ MeV, with the contribution of high-lying isoanalogous state being quite significant, so that its inclusion is necessary (this shifts the level down by about 3 MeV). We will now clarify the role of ground-state correlations (term involving $s^{(+)}$ in (3) for the case of hole nuclei). By way of example, we indicate that the reaction $^{48}\mathrm{Ca}(d,p)^{49}\mathrm{Ca}$ proceeding via the excitation of a «particle» nucleus reveals three $5/2^+$ states peculiar to a neutron «hole» shell; for them, $\sum_i s_i^{(+)} = 0.129$ and $\sum_i s_i^{(+)} E_i = 0.691$ MeV. Upon the inclusion of these states, the energy of the $\{\nu 1d_{5/2}\}$ single-particle state becomes higher: $\varepsilon_{\nu 1d_{5/2}} = -17.97$ MeV. This demonstrates that even a rather small contribution from ground-state correlations leads to a significant shift of single-particle energies, always toward the energy gap between the shells. It is worth noting that, upon the inclusion of the $T = T_>$ states and of ground-state correlations, we obtain $\sum_i s_i^{(+)} + \sum_{i'} s_{i'}^{(-)} = 0.967$, which is very close to unity. Therefore, the value of $\varepsilon_{\nu 1d_{5/2}} = -17.97$ MeV seems quite reasonable.

Now we proceed to determine the energy of the $\{\nu 1d_{3/2}\}$ neutron orbital. In contrast to the $5/2^+$ levels, the $\{\nu 1d_{3/2}\}$ state in ^{47}Ca is fragmented rather weakly. The neutron pick-up reaction exhibits only one $3/2^+$ level at $E = 2.58$ MeV in the low-lying part of the spectrum ($s^{(-)} = 0.90$) and one isoanalogous level at 13.09 MeV ($s = 0.045$); this is the isoanalog of the $3/2^+$ state at 0.36 MeV in ^{47}K). At the same time, yet another $3/2^+$ state at 3.93 MeV ($s = 0.18$) is observed among low-lying levels of ^{47}K. Upon rescaling to the ^{47}Ca nucleus with respect to isofactors and energy, this corresponds to $s = 0.02$ and $E = 16.66$ MeV. Thus, we arrive at $\sum_{i'} s_{i'}^{(-)} = 0.965$ and $\sum_{i'} s_{i'}^{(-)} E_{i'} = 3.244$ MeV. As a result, we obtain $\varepsilon_{\nu 1d_{3/2}} = -13.31$ MeV without considering for ground-state correlations. Now we consider the contribution of these correlations. In the reaction $^{48}\mathrm{Ca}(p,x)^{49}\mathrm{Sc}$, a $3/2^+$ resonance at 15.876 MeV is observed according to data reported in [6, 8, 9]; this resonance is treated as the isoanalog of the $3/2^+$ level of the ^{49}Ca nucleus. Considering that a close excited $3/2^-$ state in ^{49}Sc at $E = 11.56$ MeV is an isoanalog of the ground state of the ^{49}Ca nucleus, we can easily determine the energy of the $3/2^+$ level in ^{49}Ca under consideration; it appears to be about 4.32 MeV, which is close to the value of $E = 4.282$ MeV obtained for the $3/2^+$ level of the ^{49}Ca nucleus (the spectroscopic factor being 0.017) in [10] from an analysis of the reaction $^{48}\mathrm{Ca}(\mathbf{d}, p)^{49}\mathrm{Ca}$. At a similar energy, this level appears in the compilation of Burrows [9], but not in [6] or in [8]. For the $\{\nu 1d_{3/2}\}$ state, we eventually obtained the values of

$\sum_{i'} s_{i'}^{(-)} + \sum_{i} s_{i}^{(+)} = 0.982$ and $\varepsilon_{\nu 1d_{3/2}} = -13.09$ MeV. Thus, the magnitude of spin–orbit splitting for the $\{1d\}$ neutron orbital in ^{48}Ca is $\Delta_{\rm ls}^{\nu}(1d) = 4.88$ MeV, which is much larger than the estimate (3.6 MeV) presented in [11].

Now we consider the $\{\pi 1d_{3/2}\}$ proton state. Experimental data (see, for example, [12]) indicate the excitation of only two low-lying $3/2^+$ states at $E = 0.36$ ($s = 0.97$) and 3.93 MeV ($s = 0.185$) in the proton pick-up reaction on ^{48}Ca, this corresponding to $\sum_{i'} s_{i'}^{(-)} = 1.155$ and $\sum_{i'} s_{i'}^{(-)} E_{i'} = 1.076$ MeV. At the same time, the proton stripping reaction on ^{48}Ca results in the excitation of a set of low-lying $3/2^+$ levels among the $T_<$ states of the ^{49}Sc nucleus; for them $\sum_{i} s_{i}^{(+)} = 0.0525$ and $\sum_{i} s_{i}^{(+)} E_i = 0.262$ MeV. Taking additionally into account the existence of the $3/2^+$ level at 4.272 MeV in the ^{49}Ca nucleus (see above), for which $s = 0.017$ in the neutron stripping reaction, we reveal the corresponding isoanalogous level $3/2^+$ in ^{49}Sc at $E = 15.88$ MeV ($s^{(+)} = 0.017/9 = 0.0019$). Thus, the total contribution of ground-state correlations corresponds to $\sum_{i} s_{i}^{(+)} = 0.0544$ and $\sum_{i} s_{i}^{(+)} E_i = 0.292$ MeV, while the energy of the proton $\{1d_{3/2}\}$ level is -16.18 MeV (-16.73 MeV without considering for ground-state correlations). It should be noted that, for the proton $\{1d_{3/2}\}$ orbital, the experimental value of $\sum_{i} s_{i}^{(+)} + \sum_{i'} s_{i'}^{(-)}$ is 1.209; that is, it exceeds unity. We will discuss this issue below.

The proton $\{1d_{5/2}\}$ orbital is the last $\{1d\}$ orbital. Here, the proton pick-up reaction excites nine $T = T_<$ $5/2^+$ states, for which $\sum_{i'} s_{i'}^{(-)} = 0.663$ and $\sum_{i'} s_{i'}^{(-)} E_{i'} = 3.933$ MeV (the corresponding isobaric analogs were taken into account in considering $5/2^+$ states in ^{47}Ca). The contribution of ground-state correlations is controlled by six $T = T_<$ $5/2^+$ levels in ^{49}Sc at energies lower than 12 MeV; for these levels, $\sum_{i} s_{i}^{(+)} = 0.0233$ and $\sum_{i} s_{i}^{(+)} E_i = 0.209$ MeV. In addition, it should be borne in mind that the neutron stripping reaction excites three low-lying $5/2^+$ states of ^{49}Ca that have already been taken into account in analyzing the contribution of ground-state correlations to the energy of the $\{\nu 1d_{5/2}\}$ neutron orbital in ^{47}Ca. The counterparts of these levels in ^{49}Sc are three high-lying isoanalogous levels whose energies after rescaling are 16.03, 16.23, and 17.68 MeV, with the first and the last one being observed in the ^{49}Sc spectrum at very close energies; however, their s factors were not measured in the proton stripping reaction on ^{48}Ca because of the smallness of the corresponding

isofactor. Rescaling, according to isotopic relations, the s factors of the ^{49}Ca to those of the ^{49}Sc nucleus, we obtain $\sum_i s_i^{(+)} = 0.0143$ and $\sum_i s_i^{(+)} E_i = 0.240$ MeV for these levels. As a result, we have $\varepsilon_{\pi 1d_{5/2}} = -20.43$ MeV, while the spin–orbit $\Delta_{\rm ls}^{\pi}(1d)$ splitting of the $\{1d\}$ proton orbital is 4.25 MeV, which is considerably smaller than corresponding neutron spin–orbit splitting.

The energies of other single-particle orbitals in the vicinity of the ^{48}Ca nucleus were determined in a similar way. The corresponding values are presented in Table 1.

Table 1. **Single-particle states of ^{48}Ca**

$(\nu,\pi)\, n\ell j$	$\varepsilon^{\rm exp}$	$\varepsilon^{\rm th}$(WS1)	$\varepsilon^{\rm th}$(WS2)	$\varepsilon^{\rm th}$(WS3)
$\nu 1g_{9/2}$	∼0.6	0.32	0.18	0.39
$\nu 1f_{5/2}$	–1.20	–1.97	–1.84	–2.23
$\nu 2p_{1/2}$	–2.86	–2.90	–2.85	–2.77
$\nu 2p_{3/2}$	–4.64	–5.07	–5.09	–5.01
$\nu 1f_{7/2}$	–10.23	–9.22	–9.32	–9.64
$\nu 1d_{3/2}$	–13.09	–14.03	–13.94	–14.51
$\nu 2s_{1/2}$	–13.28	–14.48	–14.48	–14.68
$\nu 1d_{5/2}$	–17.97	–18.56	–18.62	–19.02
$\pi 1g_{7/2}$	—	9.18	9.00	9.19
$\pi 2d_{5/2}$	—	3.78	3.82	3.44
$\pi 1g_{9/2}$	—	0.52	0.66	1.05
$\pi 2p_{1/2}$	–2.4	–3.07	–3.12	–3.10
$\pi 1f_{5/2}$	–3.20	–3.58	–3.70	–2.99
$\pi 2p_{3/2}$	–3.4	–5.22	–5.19	–5.18
$\pi 1f_{7/2}$	–9.40	–10.09	–9.99	–9.35
$\pi 2s_{1/2}$	–14.92	–15.87	–15.87	–15.45
$\pi 1d_{3/2}$	–16.18	–16.32	–16.39	–15.46
$\pi 1d_{5/2}$	–20.43	–20.28	–20.22	–19.46

Note. In calculations the mean-field potential (16) with the parameters $V_0 = -51.5$ MeV, $V_{\rm ls} = 33.2$ MeV$\cdot$fm^2, $r_0 = 1.27$ fm, $r_{c0} = 1.25$ fm, and $\beta = 1.39$ was used. The designation WS1 corresponds to $a = 0.6$ fm and $\beta_{\rm ls} = -0.6$; WS2 — to $a = 0.6$ fm, $\beta_{\rm ls} = -1.0$; WS3 — to diffusenesses $a(\nu) = 0.55$ fm, $a(\pi) = 0.67$ fm, and $\beta_{\rm ls} = -0.6$.

In all of the cases, with the exception of that of the $\{\pi 2p_{1/2}\}$ and $\{\pi 2p_{3/2}\}$ proton orbitals, the total experimental strength of single-particle states, which is determined by formulas (4), (11), and (12), is about unity, the spin–orbit splitting of the $1f$ proton orbital being much smaller than the neutron one. The $\{\pi 2p\}$ orbital also deserves a dedicated discussion. The compilation of experimental data concerning the proton stripping reaction on ^{48}Ca in [6] suggests an extremely strong fragmentation of the $\{\pi 2p_{1/2}\}$ state: up to an excitation energy of about

12 MeV, there are 55 ($T = T_< = 7/2$) $1/2^-$ states with the total strength $\sum_i s_i^{(+)} = 2.04$, which is twice as great as the value following from the sum rule. In addition, three very close ($T = T_> = 9/2$) $1/2^-$ levels at an energy of 13.5 MeV are observed with the total value of $\sum_i s_i^{(+)} \sim 0.1$, which correspond to the components of the energy-split isoanalog of the excited $1/2^-$ state of the ^{49}Ca nucleus at $E = 2.02$ MeV, where $s^{(+)} = 0.91$. Upon rescaling in the isofactor to the ^{49}Sc nucleus, this leads precisely to a value of about 0.1 for $s^{(+)}$. At the same time, the total strength of transitions to the $\{\pi 2p_{3/2}\}$ level — this strength receives contributions predominantly from low-lying $3/2^-$ components — is less than unity (0.682) according to [6]. Concurrently, we have $\varepsilon_{\pi 2p_{1/2}} = -2.00$ MeV and $\varepsilon_{\pi 2p_{3/2}} = -4.55$ MeV, while the proton spin–orbit splitting $\Delta^\pi_{\rm ls}(2p) = 2.55$ MeV is larger than that for neutrons ($\Delta^\nu_{\rm ls}(2p) = 1.78$ MeV).

It should be borne in mind, however, that, in the original study of Fortier et al. [13], $\{\pi 2p\}$ states were identified by the angular distribution alone, so that those authors actually determined only the value of $\ell = 1$ but not the spin of the level. It is worth noting that the $\ell = 1$ proton states in the ^{49}Sc nucleus are distributed within the interval of width about 10 MeV, which is much larger than the spin–orbit splitting of the $\{\pi 2p\}$ level. Therefore, it is reasonable to assume that $1/2^-$ and $3/2^-$ states — apart from those that are reliably identified by J^π values and which are rather low-lying and include the main components of the single-particle strength and apart from isoanalogs whose spins were determined reliably — are distributed uniformly over the spectrum. In this case $\sum s = 1.062$ and $\varepsilon \approx -3.4$ MeV for the $\{\pi 2p_{3/2}\}$ state and $\sum s = 1.38$, and $\varepsilon \approx -2.4$ MeV for the $\{\pi 2p_{1/2}\}$ level. Thus, the sum rule (3) holds to a much higher accuracy, while the proton spin–orbit splitting $\left(\Delta^\pi_{\rm ls}(2p) \approx 1 \text{ MeV}\right)$ is smaller than the spin–orbit splitting for neutrons.

Yet another comment is in order here. As can be seen from the above, the $\{\pi 1d_{5/2}\}$ proton orbital is characterized by $\sum_i s_i^{(+)} + \sum_{i'} s_{i'}^{(-)} = 0.701$, which is also smaller than unity. It could be assumed in this connection that the $3/2^+$ level at 3.93 MeV in the ^{47}K nucleus is in fact the $5/2^+$ state characterized by $s^{(-)} = 0.185 \cdot 4/6 = 0.122$. This would lead, on the one hand, to a decrease in the total strength of the $\{\pi 1d_{3/2}\}$ state to a value of 1.024 and, on the other hand, to an increase in the strength for the $\{\pi 1d_{5/2}\}$ orbital to 0.823. Concurrently, the spin–orbit splitting of the $\{1d\}$ proton orbital would increase somewhat (up to 4.80 MeV), but it would still remain smaller than that for neutrons. However, there are no sufficiently strong experimental arguments in favor of this assumption since the level in question was identified not only by the angular distribution of the cross section but also by the angular distribution of the analyzing power [14].

Therefore, the problem of the excess of the strength for the $\{\pi 1d_{3/2}\}$ state and its deficit for $\{\pi 1d_{5/2}\}$ remains open at present. Probably, it is related to the theoretical description of nucleon-transfer reactions and the possible contribution of multistep mechanisms of such reactions [12].

Summarizing all that was said in this section earlier, we would like to emphasize that an analysis of available experimental data concerning direct reactions furnishes compelling arguments in favor of the statement of the ^{48}Ca nucleus, the spin–orbit splitting of the $\{1f\}$, $\{1d\}$, and $\{2p\}$ neutron orbitals is larger than that of the analogous proton orbitals. However, it should be noted that this statement is fully valid only for $f_{5/2} - f_{7/2}$ splitting. In the case of the $\{1d\}$ orbital, we additionally invoked data on $T_>$ states, employing the (quite reliable) concept of isobaric symmetry, while, in determining the splitting of the $\{2p\}$ proton orbital, we assumed that the distribution of $1/2^-$ and $3/2^-$ levels over the «statistical» part of the spectrum is uniform.

Now we pass to the classical doubly-magic nucleus ^{208}Pb. Here, due to a strong rigidity of the core, the fragmentation of single-particle states is very weak, almost all of them have spectroscopic factors very close to unity. The exceptions are the $\{\nu 1j_{15/2}\}, \{\nu 2f_{7/2}\}$, $\{\pi 2d_{5/2}\}, \{\pi 1g_{7/2}\}$, and $\{\pi 3p_{1/2}\}$ levels, that have rather strong admixtures of the multiplet (phonon–quasiparticle) nature. The fragmentation of single-particle states at ^{208}Pb is mainly influenced by the presence of a low-lying and highly-collective 3_1^- phonon state at 2.62 MeV. The effects caused by the 2_1^+ state are less since the collectivization of quadrupole phonon, and the corresponding nucleon–phonon vertexes are small in heavy nuclei near doubly closed shells. For example, in the neutron «hole» ^{207}Pb nuclei, the main part of energy shift of the $7/2^-$ level is caused by mixing with the higher-lying $(3_1^- \otimes \nu 1i_{13/2}^{-1})_{7/2^-}$ state. Numerical evaluation performed by using the quasiparticle–phonon model with the coupling constant extracted from the $B(E3; 3_1^- \rightarrow$ ground state) value shows that the $7/2^-$ level corresponding to the «pure» $\nu 2f_{7/2}^{-1}$ state moves down by the amount of ~ 0.4 MeV, thus approaching the experimental value of 2.34 MeV. This large shift is due to rather strong coupling constant and non-spin-flip nature of the matrix element. The value of the *true* (after the procedure of averaging) energy of the $7/2^-$ state in ^{207}Pb is $10.07-7.37 = 2.7$ MeV (see Table 2). Thus, the magnitude of the predicted shift is very close to the experimental value of $2.70 - 2.34 = 0.36$ MeV mentioned above.

At the same time, the $(3_1^- \otimes \nu 1i_{13/2}^{-1})$ configuration has no $5/2^-$ component and thus one does not observe experimentally the fragmentation of the lower lying $5/2^-$ level at 0.57 MeV. We note here that the $7/2^-$ and the $5/2^-$ states in the proton «particle» ^{209}Bi nucleus have the opposite ordering, $7/2^-$ being the lower one. Due to mixing with the $(3_1^- \otimes \pi 1i_{13/2})$ configuration, the «pure» $\pi 2f_{7/2}$ level is also pushed down, but only by about 0.2 MeV due to larger energy difference. Thus, after taking account of configuration mixing, not only

the neutron $\Delta_{\rm ls}^{(\nu)}(2f)$ splitting between the pure states increased as compared to 1.77 MeV, but also the proton $\Delta_{\rm ls}^{(\pi)}(2f)$ splitting decreased to a smaller value.

The values of the «true» single-particle energies in ^{208}Pb obtained by employing the procedure of averaging over the spectroscopic factors are listed in Table 2.

Table 2. **Single-particle states of ^{208}Pb**

$(\nu,\pi)\,n\ell j$	$\varepsilon_{\rm exp}$	Stnd	Set 1	Set 2	Set 3	Set 4	SIII-1	SIII-2
$\nu 3d_{3/2}$	–1.40	–0.32	–0.02	–0.23	–0.96	–0.99	0.38	0.42
$\nu 2g_{7/2}$	–1.44	–0.79	–0.18	–0.65	–0.89	–1.14	0.01	0.14
$\nu 4s_{1/2}$	–1.90	–0.80	–0.70	–0.74	–1.63	–1.51	–0.08	–0.06
$\nu 1j_{15/2}$	–2.09*	–2.42	–3.05	–2.31	–2.23	–1.55	–1.41	–1.93
$\nu 3d_{5/2}$	–2.37	–1.50	–1.45	–1.40	–2.35	–2.13	–0.39	–0.38
$\nu 1i_{11/2}$	–3.16	–4.24	–3.37	–4.05	–2.71	–3.33	–3.37	–2.77
$\nu 2g_{9/2}$	–3.94	–3.71	–3.82	–3.59	–4.24	–3.88	–2.91	–2.97
$\nu 3p_{1/2}$	–7.37	–7.32	–6.94	–7.17	–7.59	–7.61	–7.21	–7.13
$\nu 2f_{5/2}$	–7.94	–8.42	–7.87	–8.25	–8.17	–8.38	–8.59	–8.44
$\nu 3p_{3/2}$	–8.27	–8.18	–8.03	–8.04	–8.59	–8.43	–8.18	–8.15
$\nu 1i_{13/2}$	–9.00	–9.21	–9.62	–9.08	–8.84	–8.31	–9.73	–10.21
$\nu 2f_{7/2}$	–10.07*	–10.57	–10.57	–10.43	–10.72	–10.46	–11.21	–11.24
$\nu 1h_{9/2}$	–10.78	–12.06	–11.35	–11.87	–10.60	–11.09	–13.16	–12.67
$\pi 3p_{1/2}$	0.17*	0.63	0.43	0.72	0.29	0.47	2.79	2.88
$\pi 3p_{3/2}$	–0.68	–0.45	–0.46	–0.35	–0.58	–0.69	1.99	2.03
$\pi 2f_{5/2}$	–0.97	–0.68	–1.03	–0.60	–1.03	–0.61	0.60	0.74
$\pi 1i_{13/2}$	–2.19	–2.86	–2.37	–2.71	–1.94	–2.78	–1.20	–1.53
$\pi 2f_{7/2}$	–2.90	–3.38	–3.24	–3.26	–3.21	–3.53	–1.64	–1.66
$\pi 1h_{9/2}$	–3.80	–4.60	–5.11	–4.53	–4.71	–4.01	–4.68	–4.24
$\pi 3s_{1/2}$	–8.01	–7.76	–7.86	–7.67	–7.87	–7.87	–7.39	–7.33
$\pi 2d_{3/2}$	–8.36	–8.41	–8.66	–8.32	–8.59	–8.30	–8.64	–8.51
$\pi 1h_{11/2}$	–9.36	–9.33	–8.99	–9.18	–8.60	–9.21	–9.35	–9.65
$\pi 2d_{5/2}$	–10.04*	–10.10	–10.05	–9.98	–9.96	–10.15	–10.29	–10.28
$\pi 1g_{7/2}$	–12.18*	–12.07	–12.45	–11.99	–12.08	–11.58	–13.94	–13.59

Note. The «standard» set of parameters corresponds to $V_0 = -51.50$ MeV, $V_{\rm ls} = 33.2$ MeV $\cdot$ fm^2, $\beta = \beta_{\rm ls} = +1.39$, $a(\pi) = 0.67$ fm, $a(\nu) = 0.55$ fm, and $\delta = 0.604$ MeV.

«Set 1» corresponds to $V_0 = -51.39$ MeV, $V_{\rm ls} = 33.1$ MeV $\cdot$ fm^2, $\beta = 1.43$ with $\beta_{\rm ls} = -0.6$, $a(\pi) = 0.67$ fm, $a(\nu) = 0.55$ fm fixed; $\delta = 0.654$ MeV.

«Set 2» corresponds to $V_0 = -51.34$ MeV, $V_{\rm ls} = 33.1$ MeV $\cdot$ fm^2, $\beta = 1.40$, $\beta_{\rm ls} = 1.26$ with $a(\pi) = 0.67$ fm, $a(\nu) = 0.55$ fm fixed; $\delta = 0.593$ MeV.

«Set 3» corresponds to $V_0 = -51.99$ MeV, $V_{\rm ls} = 32.7$ MeV $\cdot$ fm^2, $\beta = 1.36$, $a(\pi) = 0.73$ fm, $a(\nu) = 0.72$ fm with $\delta = 0.369$ MeV; $\beta_{\rm ls} = -0.6$ is fixed.

«Set 4» corresponds to $V_0 = -51.93$ MeV, $V_{\rm ls} = 35.2$ MeV $\cdot$ fm^2, $\beta = 1.38$, $\beta_{\rm ls} = 1.76$, $a(\pi) = 0.73$ fm, $a(\nu) = 0.72$ fm; $\delta = 0.366$ MeV.

Experimental single-particle energy marked by an asterisk ($*$) represents a mean value weighted by the spectroscopic factors.

One can see that the spin–orbit splittings of the $\{\nu 2f\}$ and $\{\nu 3p\}$ orbitals in the doubly-magic ^{208}Pb nucleus that have a large neutron excess, $N - Z = 44$, are *more* than the splittings of the analogous proton orbitals.

Recently there appeared detailed experimental information on the neutron excess nucleus ^{132}Sn that testifies to its strong magicity. In particular, in the papers [15–17] the information on the single-particle spectra of levels in odd nuclei close to ^{132}Sn was obtained. Here the important comment is necessary. The ^{132}Sn nucleus is unstable. So, by now only the data concerning the *main components* of the single-particle strength, found from the (β, γ) spectroscopy, are available. Though the existing and proposed facilities for production of beams of radioactive ions (see, for example, [18–20]) open the perspectives for measuring the spectroscopic factors «s»; in this region of a nuclidic chart, the corresponding experimental data on fragmentation are not available yet. Nevertheless, we are able to make an authentic conclusion on the relative magnitudes of the $\{\nu 2d\}$ and $\{\pi 2d\}$ spin–orbit splittings in ^{132}Sn.

To this aim, we can use the resemblance of single-particle structures at ^{132}Sn and ^{208}Pb, as well as the theoretical evaluations. Really, as was pointed out by Blomqvist [21], the ^{132}Sn and ^{208}Pb nuclei are in some respect twins, having similar shell structures with the correspondence of $l \to l + 1$, $j \to j + 1$ for most of the orbitals in these regions. Therefore, all the arguments presented above for splitting of the $\{2f\}$ levels at ^{208}Pb are completely valid also for the $\{2d\}$ states at ^{132}Sn, with replacement of $1i_{13/2}$ by $1h_{11/2}$. So far, there is no direct experimental data on the $B(E3; 3^-_1 \to \text{ground state})$ value in ^{132}Sn. However, the core has much higher rigidity here in comparison with ^{208}Pb and the energy of the 3^-_1 state is substantially higher at 4.35 MeV. Thus, from accounting for configuration mixing one expects some further increase of the $\Delta^{(\nu)}_{\rm ls}(2d)$ splitting and a decrease of $\Delta^{(\pi)}_{\rm ls}(2d)$, but these changes should be smaller than for the $\{2f\}$ levels at ^{208}Pb. Estimates based on an indirect evaluation of the $B(E3)$ value from the magnitude of the octupole effective charge in ^{134}Te [22] confirm the pattern of changes of the $\Delta^{(\pi,\nu)}_{\rm ls}(2d)$ values presented above. However, in the absence of experimental data on direct reactions we demonstrate in Table 3 the values of energies at ^{132}Sn that do not include averaging over spectroscopic factors. We see that the spin–orbit splitting of the neutron $\{2d\}$ orbital is also *more* than that for protons.

The magnitudes of spin–orbit splittings in the ^{48}Ca, ^{208}Pb, and ^{132}Sn nuclei, considered by us before, are shown in Table 4. One can see, that based on six cases described above, it is evident that the neutron spin–orbit splittings in these neutron-rich doubly closed shells nuclei are *systematically larger* than the corresponding proton splittings. Note that splittings are practically identical for protons and neutrons in the $N = Z$ nuclei, see [2], these cases are not included in Table 4.

Table 3. **Single-particle states of ^{132}Sn**

$(\nu,\pi)\,n\ell j$	$\varepsilon_{\exp}$	Stnd	Set 1	Set 2	Set 3	Set 4	SIII-1	SIII-2
$\nu 2f_{5/2}$	–0.58	0.36	0.73	0.46	0.22	–0.01	0.67	0.79
$\nu 3p_{1/2}$	(–0.92)	–0.13	–0.48	–0.09	–0.55	–0.61	0.16	0.20
$\nu 1h_{9/2}$	–1.02	–1.61	–0.84	–1.38	–0.47	–0.97	–0.72	–0.02
$\nu 3p_{3/2}$	–1.73	–0.78	–0.88	–0.77	–1.42	–1.32	–0.16	–0.14
$\nu 2f_{7/2}$	–2.58	–2.18	–2.55	–2.21	–2.84	–2.52	–1.67	–1.71
$\nu 2d_{3/2}$	–7.31	–7.74	–7.45	–7.62	–7.63	–7.77	–8.42	–8.26
$\nu 1h_{11/2}$	–7.55	–7.11	–7.96	–7.23	–7.33	–6.60	–7.69	–8.23
$\nu 3s_{1/2}$	–7.64	–7.68	–7.73	–7.64	–8.03	–7.93	–8.26	–8.21
$\nu 2d_{5/2}$	–8.96	–9.66	–9.94	–9.66	–9.98	–9.69	–10.71	–10.71
$\nu 1g_{7/2}$	–9.74	–10.56	–10.04	–10.39	–9.51	–9.81	–11.92	–11.32
$\pi 3s_{1/2}$	(–6.83)	–6.84	–6.87	–6.80	–6.64	–6.70	–4.97	–4.90
$\pi 1h_{11/2}$	–6.84	–7.32	–6.66	–7.46	–6.77	–7.48	–5.64	–6.01
$\pi 2d_{3/2}$	–7.19	–6.86	–7.20	–6.74	–7.07	–6.72	–5.93	–5.77
$\pi 2d_{5/2}$	–8.67	–9.36	–9.20	–9.37	–9.04	–9.30	–7.88	–7.88
$\pi 1g_{7/2}$	–9.63	–9.84	–10.41	–9.66	–10.60	–9.81	–10.08	–9.56
$\pi 1g_{9/2}$	–15.71	–14.91	–14.46	–15.00	–14.57	–15.02	–15.03	–15.36
$\pi 2p_{1/2}$	–16.07	–16.01	–16.22	–15.92	–16.14	–15.91	–16.68	–16.55

Note. «Stnd»: $\delta = 0.589$ MeV.

«Set 1»: $V_0 = -51.56$ MeV, $V_{\rm ls} = 33.3$ MeV $\cdot$ fm^2, $\beta = 1.39$, $\delta = 0.638$ MeV.

«Set 2»: $V_0 = -51.44$ MeV, $V_{\rm ls} = 34.8$ MeV $\cdot$ fm^2, $\beta = 1.39$, $\beta_{\rm ls} = 1.35$, $\delta = 0.575$ MeV.

«Set 3»: $V_0 = -51.55$ MeV, $V_{\rm ls} = 32.4$ MeV $\cdot$ fm^2, $\beta = 1.31$, $a(\pi) = 0.63$ fm, $a(\nu) = 0.66$ fm, $\delta = 0.546$ MeV.

«Set 4»: $V_0 = -51.56$ MeV, $V_{\rm ls} = 34.1$ MeV $\cdot$ fm^2, $\beta = 1.34$, $\beta_{\rm ls} = 1.33$, $a(\pi) = 0.65$ fm, $a(\nu) = 0.66$ fm, $\delta = 0.478$ MeV.

Table 4. **Magnitudes in MeV of neutron and proton spin–orbit splittings**

Nucleus	$n\ell$	$\Delta_{\exp}(n\ell)$, MeV	$\beta_{\rm ls}$	Nucleus	$n\ell$	$\Delta_{\exp}(n\ell)$, MeV	$\beta_{\rm ls}$
^{48}Ca	$\nu 1f$	9.02	–2.22	^{208}Pb	$\nu 2f$	2.13	–0.47
	$\pi 1f$	6.20			$\pi 2f$	1.93	
	$\nu 1d$	4.88	–0.83		$\nu 3p$	0.90	–0.27
	$\pi 1d$	4.25			$\pi 3p$	0.85	
	$\nu 2p$	1.78	–3.3	^{132}Sn	$\nu 2d$	1.65	–0.45
	$\pi 2p$	~ 1.0			$\pi 2d$	1.48	

It is thus of substantial interest to evaluate to what extent the isotopic dependence of the spin–orbit splittings is reproduced by standard model calculations. Three different approaches were made as described below.

3. THEORETICAL APPROACH

3.1. General Considerations. Turning to the theoretical interpretation [2] of the experimental values of the spin–orbit splitting discussed above, we shall first recall that from the point of view of many-body theory, the average spin–orbit potential has its origin in the pair spin–orbit interaction between nucleons (with tensor forces providing a minor contribution as well). On the level of qualitative arguments, it was noted by Bohr and Mottelson [23] that due to the symmetry properties one should expect the neutron spin–orbit splitting to be somewhat larger than that for protons in heavier nuclei, simply due to a higher number of like particles in the neutron case. However, at that time the absence of experimental data did not permit a meaningful comparison with measurements. With the presently available data we can fill this gap, providing also some quantitative considerations.

The two-body spin–orbit interaction differs from zero only in the states with a total spin $S = 1$. The neutron–neutron and proton–proton systems have the total isospin $T = 1$ and thus due to the Pauli principle have odd values of the relative orbital momentum L (in fact, $L = 1$). At the same time, the neutron–proton system is composed from the $T = 0$ and $T = 1$ states with equal weights, having $L = 0$ and $L = 1$, correspondingly. Due to the absence of spin–orbit interaction in states with $L = 0$, the pair spin–orbit np interaction is half as strong as that in pp or nn systems.

If $U_{\rm ls}(\nu)$ and $U_{\rm ls}(\pi)$ represent the magnitudes of the mean spin–orbit field for neutrons and protons and $\vartheta(T = 1, S = 1, L = 1)$ is a quantity representing the strength of the pair spin–orbit interaction in a state with $T = 1, S = 1, L = 1$, then the above discourse leads to

$$U_{\rm ls}(\nu) \sim \vartheta(1,1,1)\left(N + \frac{1}{2}Z\right) \equiv \vartheta\left(A - \frac{Z}{2}\right)$$

and

$$U_{\rm ls}(\pi) \sim \vartheta(1,1,1)\left(\frac{1}{2}N + Z\right) \equiv \vartheta\left(A - \frac{N}{2}\right). \tag{13}$$

To characterize the isotopic dependence of spin–orbit splitting we introduce the *relative difference* «ε» of the neutron and proton spin–orbit splittings

$$\varepsilon = \frac{\Delta_{\rm ls}^{(\nu)} - \Delta_{\rm ls}^{(\pi)}}{\left(\Delta_{\rm ls}^{(\nu)} + \Delta_{\rm ls}^{(\pi)}\right)/2}. \tag{14}$$

In the closure approximation $\Delta_{\ell{\rm s}}^{(\nu,\pi)} \sim U_{\rm ls}(\nu,\pi)$. Then by using formulas (13) we obtain

$$\varepsilon = \frac{2}{3}\,\frac{N-Z}{A}. \tag{15}$$

On the other side, the phenomenological average potential that generates the spectra of single-particle levels, including the spin–orbit splittings, may be represented as

$$U(r,\sigma,\tau_3) = U_0(\tau_3)f(r) + U_{\rm ls}(\tau_3)\frac{1}{r}\frac{df(r)}{dr}\hat{\mathbf{l}}\cdot\hat{\mathbf{s}} + \frac{(1+\tau_3)}{2}U_{\rm Coul},$$
$$f(r) = \left[1+\exp\left(\frac{r-R}{a}\right)\right]^{-1},\ R = r_0A^{1/3},\ R_{\rm Coul} = r_cA^{1/3}, \tag{16}$$

with the isotopic dependences of U_0 and $U_{\rm ls}$ represented in the form

$$U = V_0\left(1+\frac{1}{2}\beta\frac{N-Z}{A}\tau_3\right)$$

and

$$U_{\rm ls} = V_{\rm ls}\left(1+\frac{1}{2}\beta_{\rm ls}\frac{N-Z}{A}\tau_3\right). \tag{17}$$

Here $\tau_3 = +1$ for protons (π) and $\tau_3 = -1$ for neutrons (ν).

By now, the values of parameters entering the central part of the potential (16) are well known: $V_0 \sim -(50{-}52)$ MeV, $\beta \sim 1.4$, and $a \sim 0.6$ fm. At the same time, from the global description of spin–orbit splitting in nuclei we know the value of a spin–orbit parameter $V_{\rm ls}$ to be $V_{\rm ls} \sim +30$ MeV $\cdot$ fm^2, while the magnitude of the parameter $\beta_{\rm ls}$, that shows the isospin dependence of spin–orbit splitting, is under the question, and may be defined from the symmetry relations and from the experimental data on splittings deduced by us before.

In terms of a potential $U_{\rm ls}$ in the form (17), the magnitude of the *relative* difference of neutron and proton spin–orbit splittings is

$$\varepsilon = -\beta_{\rm ls}\frac{N-Z}{A}. \tag{18}$$

It follows from a comparison of Eqs. (15) and (18) that $\beta_{\rm ls} = -2/3$.

Strictly speaking, this derivation was performed for the two-body spin–orbit interaction. However, as mentioned above, tensor forces provide also some contribution to the spin–orbit splitting. This noncentral interaction is proportional to $\hat{S}_{12}$ with

$$\hat{S}_{12} = 3(\hat{\boldsymbol{\sigma}}_1\mathbf{n})(\hat{\boldsymbol{\sigma}}_2\mathbf{n}) - \hat{\boldsymbol{\sigma}}_1\hat{\boldsymbol{\sigma}}_2 = \sqrt{24\pi}[[\hat{\sigma}_1\otimes\hat{\sigma}_2]^2\otimes Y_2(\mathbf{n})]^0_0. \tag{19}$$

One can easily see from (19) that the diagonal matrix elements of this interaction are different from zero only for states with $S = 1$ and $L \geqslant 1$, of which the $S = T = L = 1$ one is of the main importance. It is just the state which was already considered in this subsection in the case of spin–orbit interaction.

Consequently, the diagonal part of tensor forces also provides contribution to $U_{\rm ls}$ with $\beta_{\rm ls} = -2/3$, and thus it leads only to a renormalization of the $V_{\rm ls}$ value. However, as the spatial part of tensor operator is proportional to $Y_2(\mathbf{n})$ and due to the spin structure of $\hat{S}_{12}$, this renormalization equals zero in cases of spin saturated spherical nuclei. Thus, in ^{16}O and ^{40}Ca tensor forces give a contribution to the isoscalar part of the spin–orbit splitting, that is mediated by their nondiagonal part and caused by admixtures, that are out of the Hartree–Fock type ground state. As was shown in [24], tensor forces may really lead to a substantial contribution to the isoscalar part of spin–orbit splitting. At the same time, in nuclei that are not spin saturated, such as ^{48}Ca, tensor forces can contribute to the spin–orbit splitting even in the «diagonal» scheme (i. e., a scheme without admixtures), if the, antisymmetrization is properly included. Our numerical calculations for *seniority one states* of ^{47}Ca and ^{47}K both having one neutron or proton hole and performed in the framework of the multiparticle shell model with tensor forces taken from our previous works [25–29], have demonstrated that the inclusion of a tensor component of the interaction leads to energy shifts that correspond to some variation of the spin–orbit splittings $\Delta_{\rm ls}$, such that in ^{48}Ca $\Delta_{\rm ls}^{(\nu)}(1d) - \Delta_{\rm ls}^{(\pi)}(1d) = 0.34$ MeV and $\Delta_{\rm ls}^{(\nu)}(1p) - \Delta_{\rm ls}^{(\pi)}(1p) = 0.24$ MeV. These shifts arise from neutrons filling the $\nu 1f_{7/2}$ subshell and are mainly due to charge exchange two-body matrix elements of the np interaction mediated by the isovector part of the tensor force ($\sim \hat{\boldsymbol{\tau}}_1\hat{\boldsymbol{\tau}}_2$). Thus, the inclusion of tensor forces does not change the pattern of spin–orbit splitting, which also leads to negative values of $\beta_{\rm ls}$ ranging from about -0.4 to -0.7. These results qualitatively agree with those presented in [30], where in the framework of the Brueckner–Hartree–Fock method with Reid potential (containing both the spin–orbit and tensor components), a substantially larger neutron than proton splitting was obtained for the $1p$ and $1d$ orbitals in ^{48}Ca with $\beta_{\rm ls}$ in the range from about -0.5 to -1.8. We note that if we omit the case of spin–orbit splitting of the $\pi 2p$ level in ^{48}Ca, where the experimental data on the $\Delta_{\rm ls}^{\pi}$ are rather indefinite, the average magnitude of the parameter $\beta_{\rm ls}$ as defined by formulas (14) and (18), is equal to $\beta_{\rm ls} \sim -0.85$, this value is in good agreement with the prediction $\beta_{\rm ls} = -2/3$, based on the symmetry relations (13).

3.2. Walecka Model. Here we make an evaluation of the $\beta_{\rm ls}$ parameter in the Hartree approximation starting from the Dirac phenomenology with meson–nucleon interactions according to the Walecka model [31]. It is known, that this approach enabled to explain the global magnitude of spin–orbit splitting in nuclei. Here, and mainly for heavier nuclei, we concentrate only on the *difference* between the proton and neutron splittings of spin–orbit partners in the same nuclei, and on its dependence on the value of the neutron excess in nuclei, i.e., on the isotopic dependence of splitting. In this model one obtains (see, for example, [32–39] and references therein) a Skyrme-type single-particle equation for a nucleon

having the effective mass m_N^* and subjected to the effect of a potential with the spin–orbit term having the form (see, for example, [35–38]):

$$\hat{U}_{\rm ls} = \frac{\lambda_N^2}{2}\,\frac{1}{r}\left\{\left(\frac{m_N}{m_N^*}\right)^2 \frac{d}{dr}\left[(V_\omega^0 - S_{\sigma,\sigma_0}^0) - (V_\rho^1 - S_{\delta,\sigma,\sigma_0}^1)\cdot\tau_3\right] - \right.$$
$$\left. - 2k\left(\frac{m_N}{m_N^*}\right)\frac{d}{dr}V_\rho^1\cdot\tau_3\right\}\hat{\mathbf{l}}\cdot\hat{\mathbf{s}}, \quad (20)$$

where $V = V^0 - \tau_3 \cdot V^1$ and $S = S^0 - \tau_3 \cdot S^1$ are the vector and scalar fields related to corresponding mesons, $m_N^* = m_N + \dfrac{1}{2}(S - V)$, while k is the ratio of tensor-to-vector coupling constants of ρ meson. Various approaches have been used to determine the coupling constants. In [38] the meson–nucleon coupling constants, defining the V and S fields, were taken from the Bonn NN-boson exchange potential [40], where σ and σ_0 are scalar mesons imitating the 2π exchange in the NN systems with $T = 1$ and $T = 0$, correspondingly. In other works (see, for example, [35–37]), the constants were defined from the description of global nuclear properties, with inclusion of the σ^3 and σ^4 terms in the Lagrangian density (one σ meson with the same characteristics for $T = 1$ and $T = 0$ channels was used, which leads to zero contribution of this meson to S^1 in formula (20); note also that the tensor term was not included in the ρ-meson vertex in [35–37]).

We calculate the V and S magnitudes in the center of nuclei at the values of vector and scalar densities $\rho_v = 0.17$, $\rho_s = 0.16$, $\rho_v^- = 0.17(N - Z)/A$, and $\rho_s^- = 0.16(N - Z)/A$ (all in fm^{-3}). Taking into account that the radial dependence of the (m_N/m_N^*) is much weaker than that of V and S, which are considered to be proportional to the density in the form of Fermi function, formula (20) may be approximately represented in the form (16). By using the coupling parameters from [38, 40] and taking into account the isotopic dependence of m_N/m_N^*, we obtain $V_{\rm ls} \approx 34$ MeV $\cdot$ fm^2 and $\beta_{\rm ls} \approx -0.40$. If we use the NL2 set of parameters from [36, 37], then we have $V_{\rm ls} \approx 31$ MeV $\cdot$ fm^2, $\beta_{\rm ls} \approx -0.43$. At the same time, the set NL1 from [35, 37], giving small values of effective masses, leads to $V_{\rm ls} \sim 50$ MeV $\cdot$ fm^2 and $\beta_{\rm ls} \sim -1.3$. As the V^1, S^1 magnitudes are proportional to ρ_v^- and ρ_s^-, formula (20) gives equal spin–orbit splittings for protons and neutrons in the $N = Z$ nuclei. It should be noted, that the value of $\beta_{\rm ls}$ is always negative and is determined mainly, or entirely, by the ρ-meson conribution.

We note in summary that the magnitudes of the empirical effective values of $\beta_{\rm ls}$ at ^{48}Ca, ^{132}Sn, and ^{208}Pb, listed in our previous discussion, are quite well reproduced by the calculations in this subsection, made in the framework of the Walecka model.

It is worth mentioning that a study of the neutron spin–orbit splitting in light nuclei as a function of A at given Z was recently performed in the framework of the Walecka model by Lalazissis et al. [41]. However, the intercomparison between the splittings of both proton and neutron «similar» spin–orbit doublets in the same nuclei was not performed there. At the same time, the calculations of single-particle spectra for magic nuclei with $N > Z$ performed by Rutz et al. [42] in the framework of the relativistic mean-field theory, which in principle represents the generalization of the Walecka model, lead to an inadequate result. Here, on the one hand, the calculations lead to the *greater* spin–orbit splittings for protons, than for neutrons, for similar orbitals. On the other hand, the nonauthentic experimental data on spin–orbit splittings were used in comparison with the experiment. It is evident (see also the result of [11]) that the isospin dependence of spin–orbit splitting offers the problem for the relativistic mean-field approach.

3.3. Woods–Saxon and Skyrme Models. In our previous works [25–29], calculations were made using the $V_0 = -51.5$ MeV, $r_0 = 1.27$ fm, $V_{\rm ls} = 33.2$ MeV $\cdot$ fm^2, $a(\pi) = 0.67$ fm, $a(\nu) = 0.55$ fm, and $\beta_{\rm ls} = \beta = 1.39$, which, on the average, described the spectra of single-particle states in nuclei from ^{16}O to ^{208}Pb. This set of parameters is denoted here as the «standard» one. With the appearance of new experimental data on the single-particle levels, we performed a new determination of parameter values through the Nelder–Mead method [43] by minimizing the root-mean square deviation

$$\delta = \sqrt{\frac{1}{n}\sum_{k=1}^{n}(\varepsilon_k^{\rm th} - \varepsilon_k^{\rm exp})^2}. \tag{21}$$

The computation demonstrated a very small sensitivity of results to the value of r_c, which was adopted to be the same as before: $r_c = 1.25$ fm. The minimization of δ performed for all nuclei close to ^{16}O, ^{40}Ca, ^{132}Sn, and ^{208}Pb with $r_c = 1.25$ fm and different values of r_0, showed that the minimum in all cases corresponds to $r_0 \approx 1.27$ fm, that also coincides with the value adopted by us before. The values $r_c = 1.25$ fm and $r_0 = 1.27$ fm were thus fixed in further calculations.

As was noted above, the optimal relation of proton-to-neutron spin–orbit splitting corresponds to $\beta_{\rm ls} \sim -0.6$. The fourth column, «Set 1», of Tables 2 and 3 presents the values of theoretical energy levels obtained in the optimization with fixed values of $\beta_{\rm ls} = -0.6$, $a(\pi) = 0.67$ fm and $a(\nu) = 0.55$ fm.

The fifth column, «Set 2», of Tables 2 and 3 presents the results of optimization with only two fixed parameters: $a(\pi) = 0.67$ fm and $a(\nu) = 0.55$ fm.

The values of «Set 3» correspond to an optimization at fixed $\beta_{\rm ls} = -0.6$, while «Set 4» are the results with no parameters fixed.

We see that the optimized values of V_0, $V_{\rm ls}$, and β (see formula (16)) are very close to the «standard» ones, with small variations from nucleus to nucleus. The magnitudes of the diffusinesses «a» vary more strongly, differing by about 10 to 15% from their «standard» values. A comparison of the «Stnd» with «Set 1» and of «Set 3» with «Set 4» results shows that the contribution of $\beta_{\rm ls}$ to the root-mean square deviation δ is small. It is thus more reasonable to define $\beta_{\rm ls}$ not from a minimization of δ, but rather by using the experimental and theoretical arguments mentioned above. This conclusion is confirmed by the results of Koura and Yamada [44], who made a number of different fits of WS parameters to the same set of experimental data, obtaining diverse (in magnitude and sign) values of the parameter that defines the contribution to the spin–orbit term, which is linear in $(N-Z)/A$. A global adjustment of WS parameters simply appears to be only weakly sensitive to details of the spin–orbit splitting.

The results of the calculations presented in Tables 1 to 3 include some levels having positive energies, i.e., unbound but sub-barrier states. In such cases we present here the real part of the single-particle energies only for those states having very small decay widths.

To summarize this evaluation, we have determined the parameters of the WS potential using a global mean square-root optimization, except for the isospin-dependent spin–orbit term, where the parameter value was found to be insensitive to the adjustment. Hence the value of $\beta_{\rm ls} \sim -0.6$ was deduced from physical considerations based on experimental spin–orbit splittings.

One should point out that the sign of the isospin spin–orbit term in the Woods–Saxon potential is in agreement with the sign of an analogous term present in the expression for the central nuclear potential in the Walecka model. While the spin–orbit term in this model is defined, very approximately, by the $(V-S)$ combination of the entering fields, the central nuclear potential is proportional to the $(V+S)$ combination. The main, isoscalar, part of the $(V-S)$ term is positive and the addition of an isovector contribution, arising from V^1, leads, for the $N>Z$ nuclei, as was shown above by us, to an additional term (positive for neutrons and negative for protons), its magnitude growing with $(N-Z)$, together with the ratio of neutron-to-proton splittings. At the same time, the isoscalar part of the central $(V+S)$ term is negative. The addition of a V^1 term leads here, for neutrons in $(N>Z)$ nuclei, to reduction of the absolute value of $(V+S)$. So, with increasing N at a given Z, the depth of the central nuclear potential for neutrons decreases and they become less bound, while the protons become more bound. All this is reflected in the WS model (see Eq. (16) above) by the fact that $\beta_{\rm ls}$ is negative, while β is positive. The two models are thus fully consistent in this respect.

As another model approach, which complements the aforementioned evaluations, we have consider the Hartree–Fock calculations with the Skyrme SIII interaction. The results of these self-consistent calculations, listed in the last two

columns of Tables 2 and 3, were obtained by considering the contribution of a single-particle part of the center-of-mass energy and taking into account the Coulomb exchange term in the Slater approximation. The SIII-1 results correspond to calculations which take into account all terms of the energy functional contributing to spin–orbit splitting, while the SIII-2 results have been obtained by omitting the spin density terms in the spin–orbit potential. In the last case our results are close to those from the study by Leander et al. [45] performed for ^{208}Pb and ^{132}Sn nuclei. We see that the results obtained in the framework of the Hartree–Fock method also demonstrate that the calculated neutron spin–orbit splittings of the $2d$ orbit in ^{132}Sn as well as of the $2f$ and $3p$ orbits in ^{208}Pb are larger than for protons and they correspond to effective $\beta_{\rm ls}$ in the interval from -0.9 to -0.6. We note that the difference between the neutron and proton spin–orbit splittings is reproduced here by using a simple parameterization of the Skyrme forces. Our calculated results differ from those of Noble [33] who declared that the isotopic dependence of the spin–orbit potential in the Hartree scheme is cancelled through the contribution of exchange terms, but agree with that of [30]. We mention here that the SIII parameterization contains density-dependent terms that imitate in some sense the three-body interaction.

4. POLARIZATION EFFECTS IN (p, n) REACTIONS PROCEEDING BETWEEN THE ISOBARICAL NUCLEAR STATES

In this section we shall corraborate our conclusions on the isotopic dependence of spin–orbit splitting by attracting another set of experimental data, this time on charge-exchange (p, n) reactions and by using the concept of the isobaric invariance of the mean nuclear potential.

For this aim we generalize expressions (17) for the central and spin–orbit terms of the mean nuclear potential by introducing the quantities $t_3 = -\tau_3/2$, $T_3 = (N-Z)/2$ and making in the spirit of [46] substitution $T_3 \cdot t_3 \to \hat{\mathbf{T}} \cdot \hat{\mathbf{t}}$, where $\hat{\mathbf{T}}$ and $\hat{\mathbf{t}}$ are isospin vector operators for the core and the nucleon. Thus, we obtain the nuclear part of potential (16) in the isobaric-invariant form (Lane potential), suitable for description of both the diagonal in t_3 (single-particle spectra and elastic scattering) and nondiagonal ((p, n) reactions leading to isobaric analogous states) processes:

$$\hat{U} = V_0 \left(1 - 2\beta \frac{\hat{\mathbf{T}} \cdot \hat{\mathbf{t}}}{A}\right) f(r) + V_{\rm ls} \left(1 - 2\beta_{\rm ls} \frac{\hat{\mathbf{T}} \cdot \hat{\mathbf{t}}}{A}\right) \frac{1}{r} \frac{df}{dr} \hat{\mathbf{l}} \cdot \hat{\mathbf{s}}. \tag{22}$$

A spin–orbit term in a potential leads to polarization effects in scattering. We see from (22) that while the polarization in elastic scattering depends on the parameter combination of the form $V_{\rm ls}\left(1 - \beta_{\rm ls} \dfrac{(N-Z)}{A} t_3\right) \approx V_{\rm ls}$, similar effects in

charge-exchange reactions with excitation of isoanalogous states are proportional to $\beta_{\rm ls} \cdot V_{\rm ls}$, and are thus defined by the isovector mean spin–orbit field parameter $\beta_{\rm ls}$, as the $V_{\rm ls}$ parameter is well known. Thus, we can check our previous conclusions concerning the $\beta_{\rm ls}$ value and based on nuclear spectra using the data from (p,n) quasi-elastic scattering. Exactly, we consider the charge-exchange (p,n) process happening between the ground state $\left(T^{(i)} = T_z^{(i)} = (N-Z)/2\right)$ of the initial nucleus and the excited isoanalogous state $\left(T^{(f)} = T^{(i)} = (N-Z)/2,\right.$ $\left. T_z^{(f)} = (N-Z)/2 - 1\right)$ of the final nucleus; this nondiagonal in t_3 process is just described by the potential (22).

Before we carefully studied the splitting of the proton and the neutron spin–orbit doublets in ^{48}Ca. The experimental information on the polarization effects in the ^{48}Ca region is available in [47], where the ^{48}Ca(p,n) ^{48}Sc reaction with polarized protons leading to the 0^+ (6.67 MeV) isoanalogous state was studied.

For checking the isobaric structure of the 6.67 MeV excited state in ^{48}Sc we performed the RPA calculations [1] in the charged particle–hole channel. This approximation was successfully used by us before in describing the particle–hole nuclei ^{208}Bi, ^{208}Tl, ^{132}Sb, and ^{132}In (see [25, 48], where all of the required formulas can be found). We started from the two-body effective interaction

$$\hat{\vartheta} = \exp\left(-\frac{r^2}{r_{00}^2}\right)\Big(V + V_\sigma \hat{\boldsymbol{\sigma}}_1\hat{\boldsymbol{\sigma}}_2 + V_T\hat{S}_{12} + V_\tau\hat{\boldsymbol{\tau}}_1\hat{\boldsymbol{\tau}}_2 + \\ + V_{\tau\sigma}\hat{\boldsymbol{\sigma}}_1\hat{\boldsymbol{\sigma}}_2\cdot\hat{\boldsymbol{\tau}}_1\hat{\boldsymbol{\tau}}_2 + V_{\tau T}\hat{S}_{12}\hat{\boldsymbol{\tau}}_1\hat{\boldsymbol{\tau}}_2\Big), \quad (23)$$

which was introduced in our previous papers [25–29]. The parameters in (23) were set to $V = -9.95$, $V_\sigma = 2.88$, $V_T = -1.47$, $V_\tau = 5.90$, $V_{\tau\sigma} = 4.91$, $V_{\tau T} = 1.51$ (all of these values are given in MeV), and $r_{00} = 1.8$ fm (interaction version 1). We also used a basis consisting of 13 proton and 11 neutron orbitals closest to the Fermi surface (and involving a set of quasi-stationary states), with the energies of the orbitals corresponding to the WS1 parameter set, see Table 1. The calculated energies of levels in the ^{48}Sc nucleus are given in Table 5, along with relevant experimental data. For all of the levels presented in Table 5 (with the exception of the 1_2^+ state), the leading configuration is $\{\pi 1f_{7/2}\overline{\nu 1f_{7/2}}\}$. As far as the 1_2^+ state is concerned, it corresponds to a Gamow–Teller resonance that manifests itself as a rather wide peak in the energy range of 5–14 MeV, with its maximum being at about 10 MeV; its leading configuration is $0.97\{\pi 1f_{5/2}\overline{\nu 1f_{7/2}}\} + 0.22\{\pi 1f_{7/2}\overline{\nu 1f_{7/2}}\}$ with $B(\mathrm{GT}; 0_1^+ \to 1_2^+) \sim 19$. At the same time, the 1_1^+ level is characterized by the structure $0.97\ \{\pi 1f_{7/2}\overline{\nu 1f_{7/2}}\}$ – $0.22\ \{\pi 1f_{5/2}\overline{\nu 1f_{7/2}}\}$ and by a value of $B(\mathrm{GT}; 0_1^+ \to 1_1^+) \sim 5$. For the 0_1^+ state, the calculated value of the reduced probability is $B(F; 0_1^+ \to 0_1^+) \simeq 7.99$, which saturates almost completely the sum rule for a transition of the Fermi type, this

state thus indeed offers the isoanalog of the ground state of the core nucleus ^{48}Ca. In Table 5, we also present the results of calculations that employ a somewhat modified interaction (version 2), where (as compared to (23)) $V_\tau = 7.9$ MeV and $V_{\tau\sigma} = 5.9$ MeV. In this case, the agreement with experimental data on energies becomes better, while the values of $B(F)$ and $B(\mathrm{GT})$ undergo virtuality no changes. It should be noted that, while the calculated energies of the levels are by and large in good agreement with the experimental data, the calculated energy of the 7_1^+ state proves to be rather low, but it is close to the energy 0.39 MeV of a low-lying level which spin is not identified. It should be emphasized, however, that experimental data cast some doubt on the existence of this level, while the 7_1^+ state at 1.10 MeV was observed in a few independent studies.

Table 5. **Experimental and theoretical energy levels of ^{48}Sc**

J^π	E^{exp}	E^{th} (Var.1)	E^{th} (Var.2)
6_1^+	gr. st.	gr. st.	gr. st.
5_1^+	0.13	0.18	0.20
4_1^+	0.25	0.18	0.22
3_1^+	0.62	0.56	0.65
7_1^+	1.10	0.42	0.44
2_1^+	1.14	0.89	1.07
1_1^+	2.52	2.04	2.36
0_1^+	6.67	4.88	6.41
1_2^+	5–14	9.44	9.95

It should also be noted that the calculated energies of other levels in ^{48}Sc, which are not quoted in Table 5 and which are associated with high-lying (for example, $\{\pi 1f_{5/2}\,\overline{\nu 1f_{7/2}}\}$) particle–hole configurations, appear to be above 3.5 MeV. In addition to the possible level at 0.39 MeV, other states manifest themselves in experiments from an energy value as low as some 1.5 MeV. Evidently, they are of more complicated nature and are caused by a weak magicity of the core nucleus ^{48}Ca, as was mentioned above in discussing the spectroscopic factors of odd nuclei in the vicinity of the ^{48}Ca. These levels can be explained in terms of pairing correlations in the ground state of the ^{48}Ca nucleus.

In [47], the theoretical analysis of the $^{48}\mathrm{Ca}(p,n)^{48}\mathrm{Sc}$ reaction was based on the microscopic approach for description of nuclear structure and in terms of the «free» nucleon–nucleon amplitudes (DWIA). Here we proceed in terms of the Lane model basing on spin–orbit parameters defined in [2] and using the Born approximation for description of scattering. Similar effects but for other target nuclei were also studied in this approach in [49].

It is well known that in the Born approximation polarization effects arising from the spin–orbit potential disappear [50]. Thus for description of them one

needs to introduce imaginary part (absorption) into the optical potential, that really means the account of effects out of the Born approach. We must also include in real and imaginary parts of potential the dependence on the incident energy, that was rather high ($T = 134$ MeV) in [47]. In [23, 51], the following proposition in the case of volume absorption is presented for the V_0 parameter: $V_0 = V_0'(1 - 0.0058T)$ with $V_0' = -52$ MeV, that is rather close to the value of -51.5 MeV obtained by us in [2]. In this case the corresponding absorption term in the optical potential was proposed in [51] in the form of $i \cdot W_V f(r)$ with $W_V(\text{MeV}) = -3.3(1 + 0.03T)$. Surface absorption is usually presented as $i \cdot W_S(df/dr)$. For small values of transferred momentum (small angles), both the variants of absorption must result in similar description of the scattering process. In the case of $a \ll R$ this leads to $W_S \approx -(R/3)W_V$. So, as an absorption term we use the combination of the form

$$i \cdot W_V \left[\alpha - (1-\alpha)\frac{R}{3}\frac{d}{dr}\right] f(r) \tag{24}$$

with $0 \leqslant \alpha \leqslant 1$, that leads to polarization effects, independent of α at small scattering angles, but strongly dependent on α at large values of transferred momentum. Thus, for description of polarization effects we use the optical potential of the form (22), but with

$$V_0 \to -51.5(1 - 0.0058T) - i \cdot 3.3(1 + 0.03T)\left[\alpha - (1-\alpha)\frac{R}{3}\,\frac{d}{dr}\right], \tag{25}$$

adopting similar energy dependences for isoscalar and isovector terms of central nuclear potential.

In Fig. 5, one can see the results of our calculations for the analyzing power A,

$$A_{\text{th}} = \frac{d\sigma_{\uparrow\uparrow}/d\omega - d\sigma_{\uparrow\downarrow}/d\omega}{d\sigma_{\uparrow\uparrow}/d\omega + d\sigma_{\uparrow\downarrow}/d\omega}; \quad |A| \leqslant 1 \tag{26}$$

together with experimental data and results of microscopical calculations from [47]. In formula (26), $\sigma_{\uparrow\uparrow}$ and $\sigma_{\uparrow\downarrow}$ are cross sections with the polarization vector $\boldsymbol{\varepsilon}$ of the incident protons parallel or antiparallel to $[\mathbf{k}_i \times \mathbf{k}_f]$. We see that in the case of surface absorption ($\alpha = 0$) our calculations that use the corresponding spin–orbit parameters from [2] demonstrate good agreement with the experiment up to the high values of the scattering angle. In any case, the obtained results unanimously point to the considerable contribution of the surface absorption ($(1 - \alpha) \gtrsim 0.5$) in nuclei. At the same time, introduction of the energy dependence into the spin–orbit parameter V_{ls}, analogous to that for the central nuclear field, leads to poor agreement with the experiment on the analyzing power. Satisfactory description of the cross section for the (p, n) reaction leading to isoanalogous state manifests the correct parameterization of the energy dependence of isovector terms in the central nuclear potential used by us.

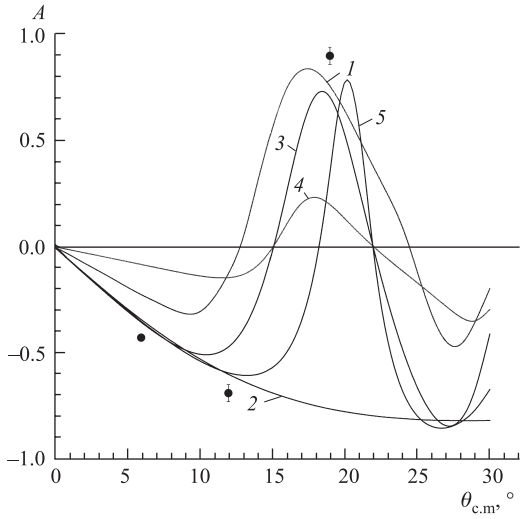

Fig. 5. Experimental data on analyzing power [47] together with results of different calculations: *1* — DWIA microscopical calculation [47]; *2* — our calculation with $\alpha = 1$ (volume absorption), $V_{\rm ls} = 33.2$ MeV $\cdot$ fm^2, $\beta_{\rm ls} = -0.6$; *3* — our calculation with $\alpha = 0$ (surface absorption), $V_{\rm ls} = 33.2$ MeV $\cdot$ fm^2, $\beta_{\rm ls} = -0.6$; *4* — our calculation with $\alpha = 0$, $\beta_{\rm ls} = -0.6$, and energy-dependent parameter $V_{\rm ls}$; *5* — the same as *2*, *3*, but with $\alpha = 0.5$; • — experiment

Our calculations with $\alpha = 0$ give the magnitude of differential cross section for the ^{48}Ca(p, n) ^{48}Sc* (I.A.S.) reaction on unpolarized protons at zero angle equal to ~ 7.7 mb/sr, very weakly increasing with the increase of the parameter «α», this cross section sharply diminishes with the increase of the scattering angle and has some structure at $\theta_{\rm c.m} \approx 20^\circ$. The value presented above may be compared with the magnitude of cross section at zero angle measured in [52] (~ 7 mb/sr), as well as with theoretical prediction [52] based on microscopical theory (~ 7.5 mb/sr).

5. SUMMARY AND CONCLUSIONS

The aforesaid results allow us to make the following conclusions:

• Using theoretical analysis and systematics of available experimental data, we have derived formula (17) that describes the *difference* between the neutron and proton spin–orbit splittings, i.e., the isotopic dependence of the mean-field spin–orbit splitting. The splitting becomes larger for neutrons than for protons

in nuclei having $N > Z$. The general arguments presented initially (based on the properties of the two-body spin–orbit and tensor interactions) gave a result in fair agreement with the empirical observations. A further microscopic study within the Walecka model supports this initial result, while it was found that a global fit of Woods–Saxon model parameters appears to be rather insensitive to the isotopic dependence of the spin–orbit splitting. A self-consistent calculation using the SIII interaction gave results in general agreement with the experiment and prediction by Eq. (17) with negative values of $\beta_{\rm ls} \sim -0.6$.

• Experimental data on the isotopical dependence of spin–orbit splitting in nuclei are consistent with the data on the (p, n) quasi-elastic scattering. The mean-field parameters $\beta_{\rm ls}$, that describe the proton and neutron spin–orbit splittings at ^{132}Sn, ^{208}Pb, and ^{48}Ca, well reproduce experimental data on polarization effects in the (p, n) quasi-elastic scattering with excitation of the isoanalogous states. Good description of analyzing power at high energy of incident protons with the spin–orbit parameters borrowed from low energy spectroscopy is consistent with supposition about the weak energy dependence of the aforementioned parameters that enter the optical model.

The isotopic dependence of the spin–orbit splitting has also been studied with methods somewhat different than those used here. In the work of Mairle [53], the average spin–orbit potential was obtained as a convolution with proton and neutron densities taken in the ratio defined by the short-range two-body spin–orbit interaction. However, the isotopic dependence of the average spin–orbit potential was not derived here in an explicit form. This point has some importance, since our analysis, based on the existing empirical data and different theoretical approaches, resulting in a simple expression, immediately shows that the difference between the neutron and proton splittings becomes saturated at large N, which precludes very large differences. The rather modest difference with a magnitude of about 10% seen in the ^{132}Sn region is already about 25% of the saturation value, suggesting that the isospin dependence in itself is unlikely to lead to dramatic structural changes. However, in cases of extreme neutron excess, when the difference between neutron and proton spin–orbit splittings approaches the maximum value of about 40% (corresponding to several hundreds of keV), a rather significant effect on the ordering of levels can be expected.

The author is grateful to K. I. Erokhina, B. Fogelberg, and H. Mach for the collaboration as well as to B. L. Birbrair, V. E. Bunakov, and V. R. Shaginyan for numerous and useful discussions concerning the problems of spin–orbit splitting in nuclei.

This work was supported by the Russian Foundation for Basic Research (Grant No. RSGSS-5788.2006.2).

REFERENCES

1. *Isakov V. I.* // Phys. At. Nucl. 2004. V. 67. P. 911.
2. *Isakov V. I. et al.* // Eur. Phys. J. A. 2002. V. 14. P. 29.
3. *Isakov V. I.* // Phys. At. Nucl. 2003. V. 66. P. 1239.
4. *Birbrair B. L., Ryazanov V. I.* // Phys. At. Nucl. 2000. V. 63. P. 1753.
5. *Migdal A. B.* Theory of Finite Fermi Systems and Applications to Atomic Nuclei. M.: Nauka, 1982.
6. http://www-nds.iaea.or.at/
7. *Audi G., Wapstra A. H., Thibalt C.* // Nucl. Phys. A. 2003. V. 729. P. 337.
8. *Burrows T. W.* // Nucl. Data Sheets. 1995. V. 76, No. 2. P. 191.
9. *Burrows T. W.* // Nucl. Data Sheets. 1986. V. 48, No. 4. P. 569.
10. *Abegg R., Hutton J. D., Williams-Norton M. E.* // Nucl. Phys. A. 1978. V. 303. P. 121.
11. *Ren Z., Toki H.* // Progr. Theor. Phys. 2002. V. 104. P. 595.
12. *Ogilvie C. A. et al.* // Nucl. Phys. A. 1987. V. 465. P. 445.
13. *Fortier S., Hourani E., Maison J. M.* // Nucl. Phys. A. 1980. V. 346. P. 285.
14. *Banks S. M. et al.* // Nucl. Phys. A. 1985. V. 437. P. 381.
15. *Hoff P. et al.* // Phys. Rev. Lett. 1996. V. 77. P. 1020.
16. *Sanches-Vega M. et al.* // Phys. Rev. Lett. 1998. V. 80. P. 5504.
17. *Stone N. J. et al.* // Phys. Rev. Lett. 1997. V. 78. P. 820.
18. *Radford D. C. et al.* // Proc. of the Intern. Symp. on Frontiers of Collective Motions (CM2002), Aizu, Japan, Nov. 6–9, 2002. P. 318.
19. An International Accelerator Facility for Beams of Ions and Antiprotons. Conceptual Design Report. GSI Report. 2001.
20. The Sixth Intern. Conf. on Radioactive Nuclear Beams (RNB6), Argonne, USA, Sept. 22–26, 2003; http://www.phy.anl.gov/rnb6
21. *Blomqvist J.* // Proc. of the 4th Intern. Conf. on Nuclei Far from Stability, Helsingor, 1981; CERN Report. 1981. V. 81-09. P. 536.
22. *Omtvedt J. P. et al.* // Phys. Rev. Lett. 1995. V. 75. P. 3090.
23. *Bohr A., Mottelson B. R.* Nuclear Structure. N. Y.; Amsterdam: W. A. Benjamin, 1969. V. 1.
24. *Pieper S. C., Pandharipande V. R.* // Phys. Rev. Lett. 1993. V. 70. P. 2541.
25. *Erokhina K. I., Isakov V. I.* // Phys. At. Nucl. 1994. V. 57. P. 198.
26. *Erokhina K. I., Isakov V. I.* // Phys. At. Nucl. 1996. V. 59. P. 589.
27. *Erokhina K. I. et al.* Preprint PNPI, No. 2225. Gatchina, 1998.
28. *Erokhina K. I. et al.* // Part. Nucl., Lett. 2001. No. 4[107]. P. 5.
29. *Isakov V. I., Erokhina K. I.* // Phys. At. Nucl. 2002. V. 65. P. 1431.
30. *Davies K. T. R., McCarthy R. J.* // Phys. Rev. C. 1971. V. 4. P. 81.
31. *Walecka J. D.* // Ann. Phys. 1974. V. 83. P. 491.
32. *Brockmann R.* // Phys. Rev. C. 1978. V. 18. P. 1510.
33. *Noble J. V.* // Nucl. Phys. A. 1979. V. 329. P. 354.

34. *Birbrair B. L., Savushkin L. N., Fomenko V. N.* // Sov. J. Nucl. Phys. 1982. V. 35. P. 664.
35. *Reinhardt P. G. et al.* // Z. Phys. A. 1986. Bd. 323. S. 13.
36. *Lee Suk-Joon et al.* // Phys. Rev. Lett. 1986. V. 57. P. 2916.
37. *Koepf W., Ring P.* // Z. Phys. A. 1991. Bd. 339. S. 81.
38. *Birbrair B. L.* Preprint PNPI, No. 2234. Gatchina, 1998.
39. *Yoshida S., Sagawa H.* // Nucl. Phys. A. 1999. V. 658. P. 3.
40. *Macleidt R., Holinde K., Elster Ch.* // Phys. Rep. 1987. V. 149, No. 1. P. 1.
41. *Lalazissis G. A. et al.* // Phys. Lett. B. 1998. V. 418. P. 7.
42. *Rutz K. et al.* // Nucl. Phys. A. 1998. V. 637. P. 67.
43. *Nelder J. A., Mead R.* // Comp. J. 1967. V. 7. P. 308.
44. *Koura H., Yamada M.* // Nucl. Phys. A. 2000. V. 671. P. 96.
45. *Leander G. A. et al.* // Phys. Rev. C. 1984. V. 30. P. 416.
46. *Lane A. M.* // Nucl. Phys. 1962. V. 35. P. 676.
47. *Anderson B. D. et al.* // Phys. Rev. C. 1986. V. 34. P. 422.
48. *Artamonov S. A. et al.* // Sov. J. Nucl. Phys. 1982. V. 36. P. 486.
49. *Gosset J., Mayer B., Escudie J. L.* // Phys. Rev. C. 1976. V. 18. P. 878.
50. *Landau L. D., Lifshits E. M.* Quantum Mechanics. M.: Fizmatgiz, 1963 (in Russian).
51. *Sitenko A. G.* Theory of Nuclear Reactions. M.: Energoatomizdat, 1983 (in Russian).
52. *Anderson B. D. et al.* // Phys. Rev. C. 1985. V. 31. P. 1147.
53. *Mairle G.* // Z. Phys. A. 1995. Bd. 350. S. 285.